HHS Public Access

Author manuscript

*Int Forum Allergy Rhinol*. Author manuscript; available in PMC 2017 February 21.

Published in final edited form as:

*Int Forum Allergy Rhinol*. 2015 December ; 5(12): 1141–1150. doi:10.1002/alr.21634.

# Topical Cathelicidin (LL-37) an Innate Immune Peptide Induces Acute Olfactory Epithelium Inflammation in a Mouse Model

**Jeremiah A. Alt, MD, PhD**[*,1,3], **Xuan Qin, MS**[1], **Abigail Pulsipher, PhD**, **Quinn Orb, BS**[1], **Richard R. Orlandi, MD**[1], **Jianxing Zhang, PhD**[3], **Austin Schults, BS**[2], **Wanjian Jia, MD, PhD**[2], **Angela P. Presson, PhD**[4], **Glenn Prestwich, PhD**[*,3], and **Siam Oottamasathien, MD**[*,2,3]

[1]Division of Head and Neck Surgery, Rhinology - Sinus and Skull Base Surgery Program, Department of Surgery; University of Utah School of Medicine, Salt Lake City, Utah, USA

[2]Division of Pediatric Urology, Department of Surgery; University of Utah School of Medicine, Salt Lake City, Utah, USA

[3]Department of Medicinal Chemistry and Center for Therapeutic Biomaterials, Salt Lake City, Utah, USA

[4]Division of Epidemiology, Department of Internal Medicine, University of Utah, Salt Lake City, Utah, USA

## Abstract

**Background—**Cathelicidin (LL-37) is an endogenous innate immune peptide that is elevated in patients with chronic rhinosinusitis (CRS). The role of LL-37 in olfactory epithelium (OE) inflammation remains unknown. We hypothesized that 1) LL-37 topically delivered would elicit profound OE inflammation, and 2) LL-37 induced inflammation is associated with increased infiltration of neutrophils and mast cells.

**Methods—**To test our hypothesis we challenged C57BL/6 mice intranasally with increasing concentrations of LL-37. At 24 hours tissues were examined histologically and scored for inflammatory cell infiltrate, edema, and secretory hyperplasia. In separate experiments, fluorescently conjugated LL-37 was instilled and tissues were examined at 0.5 and 24 hours. To test our last hypothesis, we performed tissue myeloperoxidase (MPO) assays for neutrophil activity and immunohistochemistry for tryptase to determine the mean number of mast cells per $mm^2$.

**Results—**LL-37 caused increased inflammatory cell infiltrate, edema, and secretory cell hyperplasia of the sinonasal mucosa with higher LL-37 concentrations yielding significantly more inflammatory changes ($p < 0.01$). Fluorescent LL-37 demonstrated global sinonasal epithelial

Corresponding author: Jeremiah A. Alt, MD, PhD, University of Utah, Division of Otolaryngology – Head and Neck Surgery, 50 North Medical Drive, Room 3C120, Salt Lake City, UT 84132, Telephone: (801) 585-7143, Fax: (801) 585-5744, jeremiah.alt@hsc.utah.edu.

**Potential Conflicts of Interest:** None

[*]**Financial disclosures:** Financial interest and/or other relationship with GlycoMira Therapeutics.

Accepted for an oral presentation at the American Rhinologic Society at the annual Combined Otolaryngology Spring Meetings (COSM), April 22-26, 2015, Boston, MA., USA.

binding and tissue distribution. Further, higher concentrations of LL-37 led to significantly greater MPO levels with dose-dependent increases in mast cell infiltration ($p < 0.01$).

**Conclusions—**LL-37 has dramatic inflammatory effects in the OE mucosa that is dose-dependent. The observed inflammatory changes in the olfactory mucosa were associated with the infiltration of both neutrophils and mast cells. Our biologic model represents a new model to further investigate the role of LL-37 in OE inflammation.

### MeSH Key Words

Sinusitis; rhinosinusitis; chronic disease; innate immunity; cathelicidin

## Introduction

Chronic rhinosinusitis (CRS) is one of the most common and debilitating health conditions that afflicts millions of patients every year and has known staggering effects on morbidity and societal burden. Sinonasal inflammation is the most common etiology of olfactory loss[1] with 30 to 60 % of this patient population reporting olfactory dysfunction[2,3] and the loss of smell is used as a criterion for the diagnosis of CRS.[4] Despite the widespread prevalence of olfactory dysfunction and its significant deleterious effect on health, it is surprising how little we know about the pathogenesis of olfactory loss associated with rhinosinusitis that is due, in part, to the lack of a surrogate model of olfactory epithelium (OE) inflammation. Although the exact mechanisms remain unknown, increasing evidence implicates the innate immune system may play a role,[5,6] as the sinonasal mucosa is constantly being exposed to environmental insults that require an immune response within the epithelium.

Little is known about the underlying etiopathogenesis of CRS-associated OE inflammation. The pathophysiology of inflammation, however, may be secondary to the high expression of cathelicidin and LL-37, its post-enzymatic cleaved peptide product.[7,8] LL-37 is cytotoxic at low concentrations and can induce apoptosis, negatively impacting the inflammatory balance. Prior investigations have also shown expression of LL-37 mRNA and protein in both upper airway epithelial cell cultures and in human nasal mucosa in patients with CRS.[9] LL-37 has also been shown to trigger inflammation via stimulation of mast cell degranulation and expression, and enhanced neutrophil function, while directly regulating production of cytokines/chemokines and reactive oxygen species.[10-13] LL-37 is released into the airway,[14] implicated in the innate immune system gone awry,[15] and may be playing a significant role in OE inflammation.

Animal models have enhanced our insight into the pathophysiology of many human diseases. One of the remaining barriers to understanding sinonasal inflammation and development of new treatment strategies is an acceptable non-infectious and non-allergenic animal model that induces reproducible inflammation. Currently, animal models for inducing rhinosinusitis and OE inflammation are limited to those models that cause an inflammatory response by inoculation of bacteria or generating a chronic allergic animal model sensitized to Aspergillus fumigatus (Af),[16] or with induction of ovalbumin with Staphylococcus aureus enterotoxin B,[17] yet CRS is not considered a chronic bacterial disease nor is there strong evidence for an allergic association.[18] Other exciting new genetic

models have shown that pro-inflammatory cytokines such as tumor necrosis factor can have profound effects on OE inflammation.[19] Our model relies on neither infectious or allergic stimulus but instead builds upon prior investigations that have demonstrated elevated levels of LL-37 are associated with profound inflammation in epithelial cells of the skin,[15,20] lower airway,[14] and bladder.[21] Further, topically administered 24 amino acid peptide derivatives of LL-37 at increasing concentrations have pro-inflammatory and ciliotoxic effects on sinus mucosa in a rabbit model of sinusitis.[22] Human studies have shown LL-37 to be elevated in patients with chronic upper airway inflammation such as CRS and allergic fungal rhinosinusitis.[7,9,23] However, the inflammatory response induced by LL-37 in the upper airway has not been well studied.

Our objective was to develop a noninfectious, non-allergic mouse model of acute OE inflammation that is based off of LL-37, which is a naturally occurring peptide that is constitutively expressed and found in the upper airway. We first hypothesized that LL-37 induces OE inflammation by binding and distributing in the olfactory mucosa in a dose dependent manner. We also hypothesized that the OE inflammation mechanistically involves mast cells and neutrophils, as LL-37 is known to induce mast cell and neutrophil chemotaxis.[24,25]

## Materials and Methods

### Mouse Model of LL-37-induced Sinonasal Inflammation

Twenty-four male C57BL/6 mice were purchased from Charles River (Santa Clara, CA) and housed in pathogen free conditions at the University of Utah Laboratory of Comparative Medicine. At the time of experimentation all animals were 10-12 weeks old. All animal experiments were performed under the regulation of the Institutional Animal Care and Use Committee (IACUC) at the University of Utah. LL-37 was obtained in high performance liquid chromatography-homogenous form (peptide sequence: LLGDFFRKSKEKIGKEFKRIVQRIKDFLRNLVPRTES) and dissolved in nanopure water to yield each concentration tested, which corresponds to each experimental group (0, 80, 160 and 320 μM). The total volume delivered was always 40 μl in each nare administered as timed (10 minute intervals) and divided in volumes of 10 μl per nare every ten minutes. The concentration of LL-37 intranasally inoculated (0 - 320 μM) was selected to reflect low to moderate local physiological concentrations as previously described in rosacea (maximum 1,500 μM).[20] At the doses selected, LL-37 has been shown to elicit erythema, vascular dilatation, increased neutrophilic infiltrate, thrombosis, and hemorrhage in both the skin and bladder in a dose dependent manner.[20,21] Each treatment group consisted of 6 mice; Group 1: 0 μM of LL-37 (control group), Group 2: 80 μM LL-37, Group 3: 160 μM LL-37, and Group 4: 320 μM LL-37. After establishing isoflurane anesthesia, intranasal inoculations were performed. Prior to treatment all groups received a gentle sinus rinse with normal saline (0.9% NaCl). The inoculant was released slowly in drops that hung off the end of a micropipette tip held directly in front of the nares allowing the mouse to spontaneously breathe in the inoculant. Mice were kept supine during and following inoculations to facilitate retention in the nasal cavity.[26] The animals were observed for 24 hours for pain or discomfort and subsequently sacrificed at 24 hours.

### Tissue collection

Animals were sacrificed at 24 hours and tissue harvested based off prior investigations showing robust inflammation at 24 hours after LL-37 treatment.[21,27] Heads were bisected in a sagittal plane at the nasal septum and the mucosa evaluated for gross differences. The bisected sections were randomly assigned to either histology/immunohistochemistry or sinus tissue processing. The olfactory epithelium was carefully dissected out under the dissecting microscope for those half heads assigned to sinus tissue processing. The sinus tissue destined for protein myeloperoxidase (MPO) analysis was flash frozen in liquid nitrogen and stored at -80° Celsius (C). In a separate experiment three mice (6 half heads) were collected to determine if there were significant differences in inflammation as measured by MPO between the right and left sides. Mouse half-heads destined for immunohistochemistry (IHC) were fixed in 10% neutral-buffered formalin at room temperature for 24 hours. After rinsing with phosphate buffered saline (PBS), the half-heads were decalcified in Shandon™ TBD-2™ Decalcifier (Thermo Scientific, USA) for up to 48 hours as previously described.[19] Immediately after decalcification, each head was cross-sectioned in a coronal plane. Following the sectioning procedure, standard dehydration methods were performed using increased concentrations of alcohol (70%, 95% 100%) and xylene. Tissue sections were embedded into separate paraffin blocks with the correct dorsal-ventral orientation.

### Tissue Neutrophil (MPO) Assay

Tissues were processed and MPO assays were performed as previously described.[21] Briefly, lysis buffer composed of 200 mM NaCl, 5 mM ethylenediaminetetraacetic acid, 10 mM tris, 10% glycerin (Sigma®), and protease inhibitor cocktail (Thermo Scientific®) were added to frozen tissue samples (200 μl lysis buffer per 10 mg frozen tissue). Two centrifuge cycles were performed (1500 revolutions per minute at 4° C for 15 minutes). In order to standardize the total protein assayed from different mouse heads we used a standard bicinchoninic acid (BCA assay) (Thermo ScientificTM PierceTM). The BCA determines the total concentration of protein in each sample compared to a protein of known concentration by using colorimetric techniques. Concentrations of MPO in the tissue homogenates were determined using a quantitative sandwich enzyme linked immunosorbent assay (ELISA) according to the manufacturer's protocol (Cat#:HK210, Hycult Biotech, The Netherlands). The detection range of the assay was between 1.6 - 100 ng/mL. All samples were run in triplicate.

### Hematoxylin and Eosin (H&E) staining

To characterize the inflammatory structure and carry out the histological evaluation, standard hematoxylin and eosin (H&E) counterstaining procedures were performed. The saline group tissues were used as controls.

### Histological Scoring

OE tissue was removed and scored for inflammation as previously described.[28,29] Briefly, inflammation was assessed by light microscopic examination. The control and OE tissue were examined in a blinded fashion. All histologic samples were reviewed and scored for inflammatory cell infiltrate, secretory hyperplasia, and thickness of the lamina propria. The

grade of inflammatory cell infiltrate was quantified on a scale of none (0), minimal (1), mild (2), moderate, (3) and severe (4). This was defined as: (1) rare individual inflammatory cells within the epithelium and lamina propria; (2) mild or light cellular infiltrate of individual or occasional clusters of inflammatory cells, (3) moderate as dense infiltrate of inflammatory cells, and (4) severe or dense inflammatory infiltrate so dense as to obscure the normal architecture of the mucosa or submucosa. Lamina propria thickness was assessed between the groups with appropriate saline controls. This was scored on a scale of normal (0), minimal thickness increase (1), mild thickness increase (2), moderate thickness increase (3), and severe thickness increase (4). Similarly secretory hyperplasia was scored on a scale of none (0), minimal (1), mild (2), moderate (3) and severe (4). This was defined as: (1) minimal is defined as rare secretory cells, (2) mild as scattered areas of secretory hyperplasia, (3) moderate as extended areas of hyperplasia, and (4) severe. Minimal was defined as rare secretory cells, mild as scattered areas of secretory hyperplasia, moderate as diffuse areas of hyperplasia, and severe as diffuse areas of secretory cells coupled with secretory metaplasia of subepithelial glands such as septal glands. In each animal, scores of 5 randomly chosen fields were recorded and a total of 30 individual scores for each criterion per group were obtained.

## Spatial and Temporal Characteristics of LL-37 in Sinonasal Mucosa

LL-37 fluorescently labeled with AlexaFluor® 633 was synthesized by adding 3 mg LL-37 and 5 mg N-hydroxy-succinimide in 5 ml deionized $H_2O$ to a solution of 1 mg AlexaFluor® 633 carboxylic acid in 2 ml of dimethylformamide. The pH was adjusted to 4.75 and N,N-dimethylaminopropyl carbodiimide (5 mg) was added. The reaction mixture was stirred overnight, and dialyzed twice against 100 mM NaCl solution and once against deionized $H_2O$. The dialyzed solution was lyophilized to yield 2.5 mg LL-37 AlexaFluor® 633 bioconjugate.

LL-37 AlexaFluor® 633 bioconjugate (320 μM) was instilled intranasally as described above. Sinus tissues were harvested at thirty minutes (t = 0.5) or at 24 hours (t = 24). Tissue sections were counterstained with DAPI (4′,6-diamidino-2-phenylindole) and imaged with FV1000 Confocal IX81 microscope (Olympus).

## Immunohistochemistry for Mast Cell Tryptase and Mast Cell Counting

**Mast Cell Tryptase DAB Immunohistochemistry—**Histological sections were deparaffinized by xylene and rehydrated through decreased concentrations of alcohols (100%, 95%, 70%). Endogenous peroxidase activity was blocked with 1% hydrogen peroxide in PBS for 20 minutes. Slides were washed three times in PBS for 3 minutes each. Antigen retrieval was performed by treating tissue sections with 1:100 dilution of antigen unmask solution (Cat # 3300, Vector Laboratories, Burlingame, CA, U.S.A.) under continuous low-level microwave heat for 1 hour. To minimize non-specific antibody binding and background signal, tissues were incubated with blocking solution (5% fetal bovine serum (FBS) in PBS and 0.3% Triton™ X-100) at room temperature for 1 hour. The tissues were then incubated with a primary antibody (1:800 dilution, Mast Cell Tryptase Antibody, sc-32889, Santa Cruz Biotechnology, Inc., Santa Cruz, CA, U.S.A.) overnight at 4° C. Slides were washed with PBS followed by an incubation with a biotinylated secondary antibody (1:

2000 dilution, Goat anti-rabbit IgG-B, sc-2040, pre-adsorbed biotin conjugated, Santa Cruz Biotechnology, Inc., Santa Cruz, CA, U.S.A.) for 1 hour at room temperature. To visualize immunoreactivity, sections were incubated in DAB peroxidase substrate for 22 to 33 seconds. Negative controls included incubation with PBS in place of the primary antibody with no immunoreactivity observed. Reactions were stopped by immersion into distilled H2O, after which the tissues were counterstained and dehydrated, as previously described.[30] Immunoflourescence experiments were done with DyLight® 633 secondary antibody (goat anti-rabbit IgG, 1:800 dilution).

**Mast Cell Counting—**In order to quantify the mast cell activation profile in the tissue, five randomly chosen high power (400×) fields for each tissue chip were recorded and the number of mast cells were counted.[21] The final results are presented as mast cell numbers per $mm^2$ per sample.

### Statistical Analysis

All Likert scale and continuous variables were summarized by the mean and standard deviation. Mast cells were also summarized by median (IQR) and range. For the outcomes of severity of inflammation, lamina propria thickness, and secretory hyperplasia, there were five measurements per mouse. A linear mixed model was fit to each outcome with treatment group (with four levels: saline, LL-37 80 μM, LL-37 160 μM, and LL-37 320 μM) as the predictor and mouse ID as a random effect; to account for correlations between measures from the same mouse. From each model we report all mean pair-wise differences and 95% confidence intervals (CIs) among LL-37 and saline treatments, and the corresponding p-values adjusted for multiple comparisons using Tukey's method. For the mast cell counts, there was only one measurement per mouse, and thus we compared each LL-37 level versus saline using a Wilcoxon rank sum test. MPO and mast cells were evaluated across saline and LL-37 concentrations using an ANOVA trend test, and then all pair-wise comparisons were made adjusting p-values using Tukey's method. For all analyses, a p-value $<0.05$ indicates a statistically significant difference. Analyses were conducted using R v. 3.0.3 software.

## Results

### Sinonasal Inflammation

Intranasal LL-37 resulted in substantial changes at the gross level compared to saline treated mice (Figure 1). LL-37 caused visibly increased vascular dilatation, erythema, severe edema, and hemorrhage of the sinonasal tissue at all the doses tested (80, 160, and 320 μM) compared to controls. Gross inspection did not demonstrate substantial visible differences with increasing LL-37 concentrations. Histology confirmed the gross differences with increased inflammatory cell infiltrate, increased lamina propria thickness, and secretory hyperplasia at 80, 160, and 320 μM of LL-37. Unlike gross observations, there was a dose-dependent increase in inflammatory cell infiltrate, increased lamina propria thickness, and secretory hyperplasia (Figure 2). No evidence of inflammation was observed in controls and inflammation levels were consistent in each group.

A semi-quantitative analysis was performed by histologically scoring inflammation between the treatment groups. We observed significant increased inflammatory cell infiltrate compared to saline controls for 80, 160 and 320 μM of LL-37, furthermore, any two treatment groups were significantly different from each other ($p<0.001$) except for 160 μM LL-37 and 80 μM of LL-37 (Figure 3; Table 1). Both 160 and 320 μM of LL-37 demonstrated significantly increased edema, thickening of the lamina propria, and secretory hyperplasia compared to the control (Figure 3: Tables 2-3; $p < 0.01$).

We next evaluated inflammation by looking at tissue MPO, a quantitative method to investigate neutrophil activity via the MPO enzyme in neutrophils. We found no significant difference in MPO levels between the right and left sides 24 hours after treating with 320 μM of LL-37 (data not shown). After 24 hours, tissues from controls showed minimal MPO activity (0.58 ng/mg). In LL-37 challenged sinus tissue there was a small increase (1.44 ng/mg, $p = 0.91$) with 80 μM, and (0.98 ng/ml, $p = 0.99$) with 160 μM, and a significant increase (10.04 ng/ml, $p < 0.001$) with 320 μM of LL-37. The differences in MPO levels between concentrations of LL-37 were statistically significant (ANOVA trend test $p < 0.001$), with a dramatic increase in MPO from 0 to 320 μM, 80 to 320 μM, and 160 to 320 μM of LL-37 (Figure 4).

## Mast Cell Involvement

To determine mast cell involvement in our LL-37 model, we performed IHC for mast cell tryptase using a DAB and immunofluorescence approach to increase mast cell detection. Mast cells were found throughout the OE tissue. The majority of the staining was observed within the lamina propria (Figure 5, D). Saline controls had very little mast cell tryptase visible (Figure 5, A & C). The number of visible mast cells increased in 320 μM LL-37 challenged tissues (Figure 5, B & D).

To determine if the infiltration of mast cells increased in a dose-dependent fashion we quantified mast cells in LL-37 treated and control tissue at 24 hours. Specific numbers of mast cells were determined by examining the epithelium and lamina propria. The differences in mast cell levels between concentrations of LL-37 were statistically significant (ANOVA trend test $p < 0.01$), with a dramatic increase in mast cells from 0 to 320 μM and 80 to 320 μM of LL-37 (Figure 6).

## LL-37 Showed Sinonasal Binding and Penetration

To elucidate the spatial and temporal binding characteristics of LL-37 activity in the sinonasal mucosa, we instilled 320 μM of LL-37 AlexaFluor® 633 and harvested at $t = 0.5$ and $t = 24$ after treatment. At $t = 0.5$, there is a solid coating of LL-37 AlexaFluor® 633 at the air-epithelial junction (red) with uptake of LL-37 into the serous mucus glands of the lamina propria. Very little to no staining was observed within the pseudostratified epithelium (Figure 7, A-C). At $t = 24$ hours, the air-epithelial junction was no longer coated with AlexaFluor® 633 with trace fluorescence remaining in the lamina propria (Figure 7, D-F). Further, tissues showed typical increased cellular infiltrate at $t = 24$ hours with nuclear staining more prominent in the submucosa (blue), confirming retained biologic activity of LL-37.

## Discussion

Little is known about the underlying pathophysiology of sterile nonbacterial inflammation in OE inflammation. Prior investigations have elucidated a key mechanism of sterile inflammation in other chronic inflammatory diseases to be secondary to a high expression of cationic antimicrobial peptide cathelicidin and its post-enzymatic cleaved product LL-37. Although the underlying etiology of CRS-OE inflammation is unknown, there is growing evidence it may be due to an altered innate immune response. LL-37 is constitutively expressed in the upper airway[9] and is critical to the innate host response in the sinuses,[14,22] with in vitro[31] and in vivo[22] activity against fungal [23] and antimicrobial peptides. Apart from exhibiting broad antimicrobial spectra, it is well known that LL-37 possesses several additional functions that are related to host defense. Examples of such functions are upregulation of proinflammatory cytokines, immune cell chemotaxis, endotoxin neutralization, angiogenic, and wound healing activities. These effects of LL-37 reveal a role as a mediator between the innate and adaptive immune responses. LL-37 is elevated in patients with CRS, is cytotoxic to epithelial cells at low concentrations, stimulates and attracts mast cells, and stimulates chemokine production. We hypothesized that a similar mechanism might contribute to inflammation in the OE. Our data demonstrates intranasal LL-37 has profound consequences on OE inflammation quantified by histologic changes, increased neutrophils, and mast cell numbers.

At a gross level we observed marked erythema and edema similar to changes observed in human disease. LL-37 caused increased inflammatory cell infiltrate, edema, and secretory cell hyperplasia with higher LL-37 concentrations yielding significantly more inflammatory changes. Tissue MPO assays were performed, as MPO is an important enzyme released by activated PMNs, and is therefore a good marker for inflammation. Our findings demonstrated a statistically significant increase in MPO after 320 μM of LL-37. These findings are consistent with prior investigations demonstrating that LL-37 elicits erythema, vascular dilatation, increased neutrophilic infiltrate, thrombosis, and hemorrhage in both the skin and bladder in a dose dependent manner.[20,21] This suggests increasing loads of LL-37 released may have sustained long lasting effects in the tissue. Further, in obstructed diseases such as CRS with stasis of mucus, LL-37 may remain in contact with the tissue further amplifying the inflammatory response.

LL-37 stimulates the degranulation and recruitment of mast cells,[24,32] a major effector cell in inflammation. Mast cells themselves contribute to local inflammation by activating NF-κB, followed by downstream cytokine and chemokine release,[33] which in turn increases eosinophil viability.[34] Further, LL-37 has been shown to activate and recruit eosinophils in vitro.[10,35] Early preliminary findings in our model ‘data not shown’ suggest eosinophils may also be playing a role. Eosinophils are a major inflammatory cell in eosinophilic rhinosinusitis,[36] a more severe form of sinonasal inflammation that is proving difficult to treat.[37,38] Mast cells were found throughout the OE epithelium after LL-37 treatment in a dose dependent manner. Interestingly, both LL-37 and mast cells are both highly elevated in patients with sinonasal inflammation.[9,23,39] Furthermore, there is regulated cross talk between LL-37 and mast cells, such that LL-37 can initiate mast cell activation followed by rapid mast cell-mediated degradation, which in turn mediates removal of LL-37 preventing

sustained activation[13] and cytotoxicity, which can occur at minimal concentrations in eukaryotic cells.[22] Aside from mast cell activation, increasing concentrations of LL-37 have been shown to up-regulate the production of chemokines and surface expression of chemokine receptors independent of bacterial challenge. This body of evidence has led investigators to hypothesize that LL-37 has pleiotropic properties; low levels function to protect the interface while increasing levels promote migration of immune cells, such as mast cells that can lead to uncontrolled local inflammation.[40] Therapies targeting LL-37 induced inflammation could prove to be promising.

Fluorescent labeled LL-37 demonstrated global sinonasal epithelial binding and tissue distribution. Specifically, LL-37 had robust epithelial barrier binding in addition to high levels seen in the lamina propria and serous/mucus glands seen at 1 hour after inoculation, consistent with prior investigations demonstrating rapid penetration within the bladder submucosa and uroepithelium.[30] The majority of LL-37 was cleared after 24 hours, with trace amounts seen in the serous/mucus glands of the lamina propria. This suggests that the inflammatory insult extends beyond the initial exposure as evidenced by increased neutrophils and mast cells in the tissue. Further, higher concentrations of LL-37 led to significantly greater MPO levels with dose-dependent increases in mast cell infiltration ($p < 0.01$). Further investigations into examining time points beyond 24 hours would be beneficial to determine the chronicity of the inflammation.

The mechanism by which LL-37 induces inflammation beyond mast cells in the upper airway is still under investigation. However, pattern recognition receptors (PRRs) such as Toll-Like Receptors (TLR) and the receptor for advanced glycation end products (RAGE) are receptors for LL-37 and are constitutively expressed at high basal levels in the airway. They are also linked to the physiology and pathophysiology of the chronic airway.[41] Our group has shown that LL-37 may signal through RAGE, as inhibiting LL-37 can modulate inflammation through RAGE.[27] In addition, both LL-37 and RAGE are highly elevated in patients with chronic sinonasal inflammation.[9,23] This pathway is not unique to the sinuses, as the RAGE pathway has been elucidated in many other chronic inflammatory diseases, including, but not limited to, rosacea,[27] arthritis,[42] and interstitial cystitis.[30] Further investigations are needed to define LL-37-RAGE induced upper airway inflammation.

Murine models have significant advantages over other species due to the readily available transgenic and gene knockout animals. However, studying physiology in the mouse does have limitations. Mice do not have the same sinonasal anatomic structure as humans with 2/3rds of the sinonasal mucosa in mice dedicated to olfaction, although, mice have clearly discernible anterior and posterior ethmoid sinuses, sphenoid sinuses and a true maxillary and secondary maxillary sinus.[43] Innate immune response also differs between mice and humans. LL-37 induced inflammation in the mouse model may not accurately reflect the multifactorial pathophysiology of human CRS. However, our observations demonstrating increased mucosal and stromal hypertrophy, metaplasia, and increased numbers of mast cells and neutrophils are encouraging. It is possible that the water used to dilute the LL-37 alone was contributing to the overall inflammation seen. However, the dose response increase seen in inflammation as measured by histology, MPO, and mast cells suggests that the increasing concentration of LL-37 was primarily contributing to the observed inflammation. In the

absence of a true non-infectious or non-allergic mouse model of inflammation, LL-37 induced OE inflammation is a step forward in mimicking inflammation induced by a naturally occurring peptide to better elucidate the underlying pathophysiology.

## Conclusions

LL-37 is a naturally occurring biologic peptide in the upper airway mucosa that has previously been shown to be upregulated in patients with chronic sinonasal disease. Exogenous application of LL-37 to the OE induces a profound dose dependent inflammatory response. The inflammatory response is likely secondary to increased neutrophils and mast cells. These findings represent a non-infectious, non-allergic, non-chemically induced OE acute inflammation model. Further, these results highlight the advantage of a dose-response model with potential use for investigating new anti-inflammatory therapies. Assessing the therapeutic efficacy of novel drugs at variable inflammatory severity levels would be an important step forward.

## Acknowledgments

Dr. Alt is supported by a grant from the National Institute on Deafness and Other Communication Disorders (NIDCD), Bethesda, MD., USA (R01 DC005805; PI/PD: TL Smith). Public clinical trial registration (www.clinicaltrials.gov) ID# NCT01332136. Dr. Orlandi is a consultant for Medtronic ENT (Jacksonville, FL., USA) which is not affiliated with this research.

## References

1. Loury MC. Current concepts in olfaction. Maryland medical journal. 1990; 39:921–926. [PubMed: 2233137]
2. Alt JA, Mace JC, Buniel MC, Soler ZM, Smith TL. Predictors of olfactory dysfunction in rhinosinusitis using the brief smell identification test. Laryngoscope. 2014
3. Litvack JR, Fong K, Mace J, James KE, Smith TL. Predictors of olfactory dysfunction in patients with chronic rhinosinusitis. Laryngoscope. 2008; 118:2225–2230. [PubMed: 19029858]
4. Rosenfeld RM, Andes D, Bhattacharyya N, et al. Clinical practice guideline: adult sinusitis. Otolaryngol Head Neck Surg. 2007; 137:S1–31. [PubMed: 17761281]
5. Ramanathan M Jr, Lane AP. Innate immunity of the sinonasal cavity and its role in chronic rhinosinusitis. Otolaryngol Head Neck Surg. 2007; 136:348–356. [PubMed: 17321858]
6. Lane AP, Truong-Tran QA, Schleimer RP. Altered expression of genes associated with innate immunity and inflammation in recalcitrant rhinosinusitis with polyps. Am J Rhinol. 2006; 20:138–144. [PubMed: 16686375]
7. Ooi EH, Wormald PJ, Carney AS, James CL, Tan LW. Human cathelicidin antimicrobial peptide is up-regulated in the eosinophilic mucus subgroup of chronic rhinosinusitis patients. Am J Rhinol. 2007; 21:395–401. [PubMed: 17882905]
8. Mader JS, Mookherjee N, Hancock RE, Bleackley RC. The human host defense peptide LL-37 induces apoptosis in a calpain- and apoptosis-inducing factor-dependent manner involving Bax activity. Molecular cancer research: MCR. 2009; 7:689–702. [PubMed: 19435812]
9. Chen PH, Fang SY. The expression of human antimicrobial peptide LL-37 in the human nasal mucosa. Am J Rhinol. 2004; 18:381–385. [PubMed: 15706986]
10. Tjabringa GS, Ninaber DK, Drijfhout JW, Rabe KF, Hiemstra PS. Human cathelicidin LL-37 is a chemoattractant for eosinophils and neutrophils that acts via formyl-peptide receptors. Int Arch Allergy Immunol. 2006; 140:103–112. [PubMed: 16557028]
11. Liu Q, Zheng JM, Chen JK, et al. Histone deacetylase 5 promotes the proliferation of glioma cells by upregulation of Notch 1. Molecular medicine reports. 2014; 10:2045–2050. [PubMed: 25050565]

12. Wan M, van der Does AM, Tang X, Lindbom L, Agerberth B, Haeggstrom JZ. Antimicrobial peptide LL-37 promotes bacterial phagocytosis by human macrophages. Journal of leukocyte biology. 2014; 95:971–981. [PubMed: 24550523]
13. Schiemann F, Brandt E, Gross R, et al. The cathelicidin LL-37 activates human mast cells and is degraded by mast cell tryptase: counter-regulation by CXCL4. J Immunol. 2009; 183:2223–2231. [PubMed: 19625657]
14. Bals R, Wang X, Zasloff M, Wilson JM. The peptide antibiotic LL-37/hCAP-18 is expressed in epithelia of the human lung where it has broad antimicrobial activity at the airway surface. Proc Natl Acad Sci U S A. 1998; 95:9541–9546. [PubMed: 9689116]
15. Bevins CL, Liu FT. Rosacea: skin innate immunity gone awry? Nature medicine. 2007; 13:904–906.
16. Lindsay R, Slaughter T, Britton-Webb J, et al. Development of a murine model of chronic rhinosinusitis. Otolaryngol Head Neck Surg. 2006; 134:724–730. discussion 731-722. [PubMed: 16647523]
17. Kim DW, Khalmuratova R, Hur DG, et al. Staphylococcus aureus enterotoxin B contributes to induction of nasal polypoid lesions in an allergic rhinosinusitis murine model. Am J Rhinol Allergy. 2011; 25:e255–261. [PubMed: 22185735]
18. Wilson KF, McMains KC, Orlandi RR. The association between allergy and chronic rhinosinusitis with and without nasal polyps: an evidence-based review with recommendations. Int Forum Allergy Rhinol. 2014; 4:93–103. [PubMed: 24395734]
19. Lane AP, Turner J, May L, Reed R. A genetic model of chronic rhinosinusitis-associated olfactory inflammation reveals reversible functional impairment and dramatic neuroepithelial reorganization. J Neurosci. 2010; 30:2324–2329. [PubMed: 20147558]
20. Yamasaki K, Di Nardo A, Bardan A, et al. Increased serine protease activity and cathelicidin promotes skin inflammation in rosacea. Nature medicine. 2007; 13:975–980.
21. Oottamasathien S, Jia W, McCoard L, et al. A murine model of inflammatory bladder disease: cathelicidin peptide induced bladder inflammation and treatment with sulfated polysaccharides. The Journal of urology. 2011; 186:1684–1692. [PubMed: 21855919]
22. Chennupati SK, Chiu AG, Tamashiro E, et al. Effects of an LL-37-derived antimicrobial peptide in an animal model of biofilm Pseudomonas sinusitis. Am J Rhinol Allergy. 2009; 23:46–51. [PubMed: 19379612]
23. Ooi EH, Wormald PJ, Carney AS, James CL, Tan LW. Fungal allergens induce cathelicidin LL-37 expression in chronic rhinosinusitis patients in a nasal explant model. Am J Rhinol. 2007; 21:367–372. [PubMed: 17621825]
24. Niyonsaba F, Iwabuchi K, Someya A, et al. A cathelicidin family of human antibacterial peptide LL-37 induces mast cell chemotaxis. Immunology. 2002; 106:20–26. [PubMed: 11972628]
25. De Y, Chen Q, Schmidt AP, et al. LL-37, the neutrophil granule- and epithelial cell-derived cathelicidin, utilizes formyl peptide receptor-like 1 (FPRL1) as a receptor to chemoattract human peripheral blood neutrophils, monocytes, and T cells. J Exp Med. 2000; 192:1069–1074. [PubMed: 11015447]
26. Visweswaraiah A, Novotny LA, Hjemdahl-Monsen EJ, Bakaletz LO, Thanavala Y. Tracking the tissue distribution of marker dye following intranasal delivery in mice and chinchillas: a multifactorial analysis of parameters affecting nasal retention. Vaccine. 2002; 20:3209–3220. [PubMed: 12163273]
27. Zhang J, Xu X, Rao NV, et al. Novel sulfated polysaccharides disrupt cathelicidins, inhibit RAGE and reduce cutaneous inflammation in a mouse model of rosacea. PLoS One. 2011; 6:e16658. [PubMed: 21347371]
28. Sautter NB, Delaney KL, Hausman FA, Trune DR. Tissue remodeling gene expression in a murine model of chronic rhinosinusitis. Laryngoscope. 2012; 122:711–717. [PubMed: 22294478]
29. Khalid AN, Woodworth BA, Prince A, et al. Physiologic alterations in the murine model after nasal fungal antigenic exposure. Otolaryngol Head Neck Surg. 2008; 139:695–701. [PubMed: 18984266]
30. Oottamasathien S, Jia W, Roundy LM, et al. Physiological Relevance of LL-37 Induced Bladder Inflammation and Mast Cells. The Journal of urology. 2013

31. Altman H, Steinberg D, Porat Y, et al. In vitro assessment of antimicrobial peptides as potential agents against several oral bacteria. The Journal of antimicrobial chemotherapy. 2006; 58:198–201. [PubMed: 16687459]
32. Chen X, Niyonsaba F, Ushio H, et al. Human cathelicidin LL-37 increases vascular permeability in the skin via mast cell activation, and phosphorylates MAP kinases p38 and ERK in mast cells. Journal of dermatological science. 2006; 43:63–66. [PubMed: 16600571]
33. Kim DY, Hong GU, Ro JY. Signal pathways in astrocytes activated by cross-talk between of astrocytes and mast cells through CD40-CD40L. Journal of neuroinflammation. 2011; 8:25. [PubMed: 21410936]
34. Levi-Schaffer F, Temkin V, Malamud V, Feld S, Zilberman Y. Mast cells enhance eosinophil survival in vitro: role of TNF-alpha and granulocyte-macrophage colony-stimulating factor. J Immunol. 1998; 160:5554–5562. [PubMed: 9605160]
35. Sun J, Dahlen B, Agerberth B, Haeggstrom JZ. The antimicrobial peptide LL-37 induces synthesis and release of cysteinyl leukotrienes from human eosinophils--implications for asthma. Allergy. 2013; 68:304–311. [PubMed: 23330796]
36. Soler ZM, Sauer DA, Mace JC, Smith TL. Ethmoid histopathology does not predict olfactory outcomes after endoscopic sinus surgery. Am J Rhinol Allergy. 2010; 24:281–285. [PubMed: 20819467]
37. Soy FK, Pinar E, Imre A, Calli C, Calli A, Oncel S. Histopathologic parameters in chronic rhinosinusitis with nasal polyposis: impact on quality of life outcomes. Int Forum Allergy Rhinol. 2013; 3:828–833. [PubMed: 23740777]
38. Czerny MS, Namin A, Gratton MA, Antisdel JL. Histopathological and clinical analysis of chronic rhinosinusitis by subtype. Int Forum Allergy Rhinol. 2014; 4:463–469. [PubMed: 24574266]
39. Takabayashi T, Kato A, Peters AT, et al. Glandular mast cells with distinct phenotype are highly elevated in chronic rhinosinusitis with nasal polyps. J Allergy Clin Immunol. 2012; 130:410–420 e415. [PubMed: 22534535]
40. Scott MG, Dullaghan E, Mookherjee N, et al. An anti-infective peptide that selectively modulates the innate immune response. Nature biotechnology. 2007; 25:465–472.
41. Neeper M, Schmidt AM, Brett J, et al. Cloning and expression of a cell surface receptor for advanced glycosylation end products of proteins. J Biol Chem. 1992; 267:14998–15004. [PubMed: 1378843]
42. Wenink MH, Santegoets KC, Butcher J, et al. Impaired dendritic cell proinflammatory cytokine production in psoriatic arthritis. Arthritis Rheum. 2011; 63:3313–3322. [PubMed: 21811995]
43. Jacob A, Chole RA. Survey anatomy of the paranasal sinuses in the normal mouse. Laryngoscope. 2006; 116:558–563. [PubMed: 16585859]

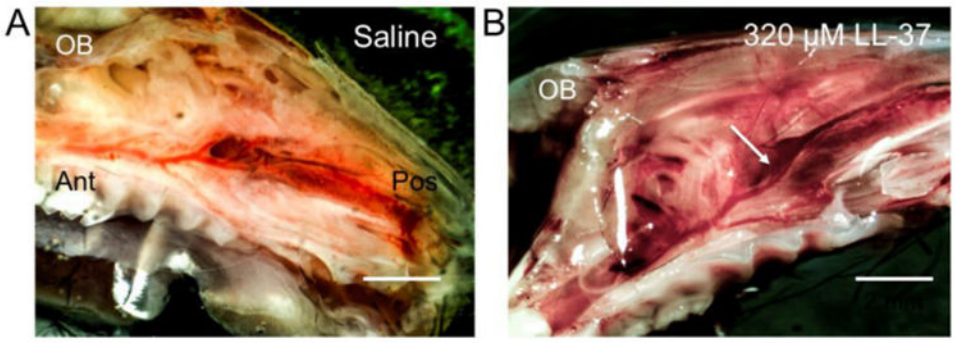


**Figure 1. Gross images of sinonasal inflammation**

Gross differences are observed in mouse hemi-sected heads demonstrating sinus mucosa (arrow) harvested 24 hours after (A) saline and (B) 320 μM LL-37 treatment. Animals treated with LL-37 (B) demonstrated increased inflammatory changes, as assessed by vascularity, erythema, hemorrhage, and edema compared to saline (A)-treated animals. Olfactory bulb (OB), posterior (Pos), anterior (Ant).

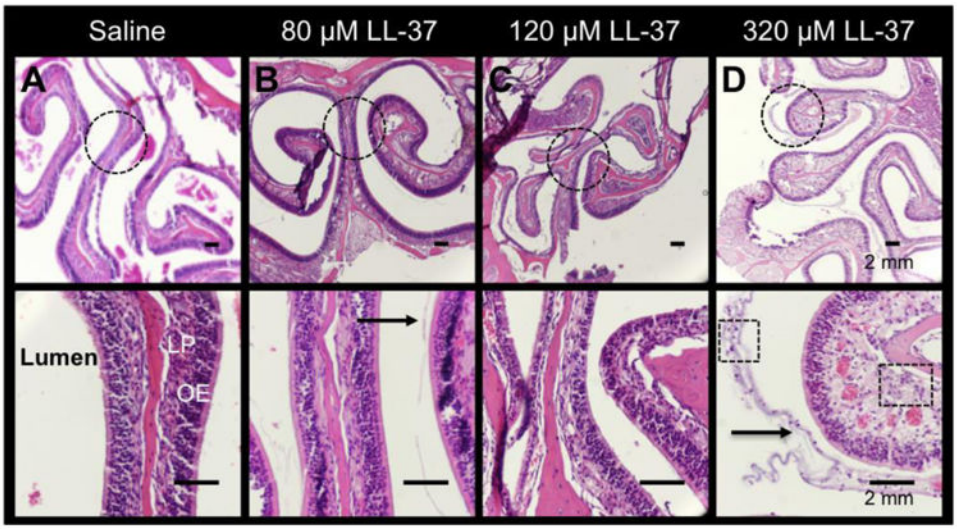


**Figure 2. LL-37 causes inflammatory changes in the olfactory epithelium in a dose-dependent manner**

H&E showing the gradual histologic changes in (A) saline, (B) 80 μM LL-37, (C) 160 μM LL-37, and (D) 320 μM LL-37. Increased inflammatory cell infiltrates (Boxes in D; magnified image), thickness of the lamina propria (LP), and mucus (arrow) are demonstrated in 320 μM LL-37-treated mice. Dotted circles are represented by the magnified images in the bottom panel.

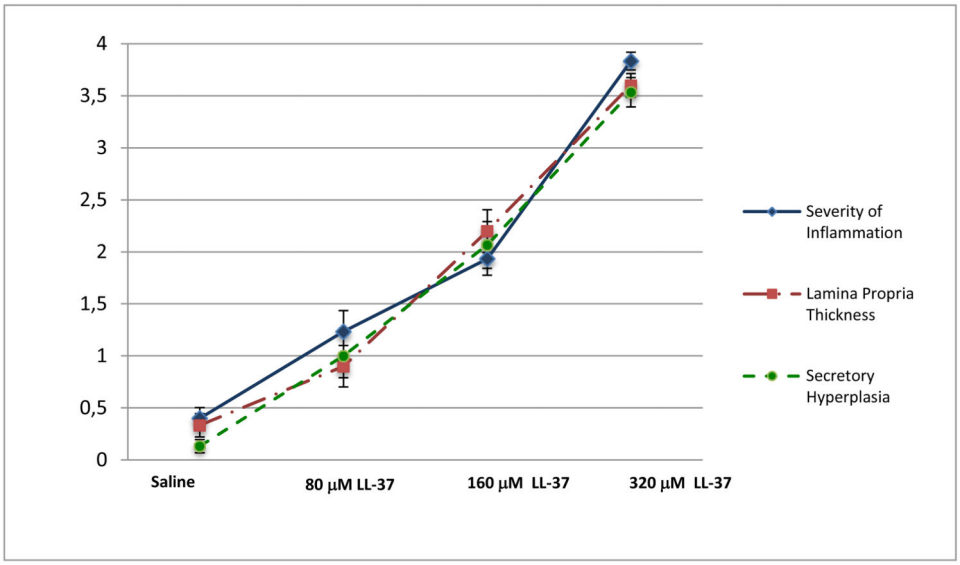


**Figure 3. Histological Scores**

The mean score and standard deviations obtained from 6 animals of four treatment groups in each category: severity of inflammation, lamina propria thickness, and secretory hyperplasia was graphed. With the 0-4 score system, each score indicates the grade of inflammation: 0 (none), 1 (minimal), 2 (mild), 3 (moderate), and 4 (severe).

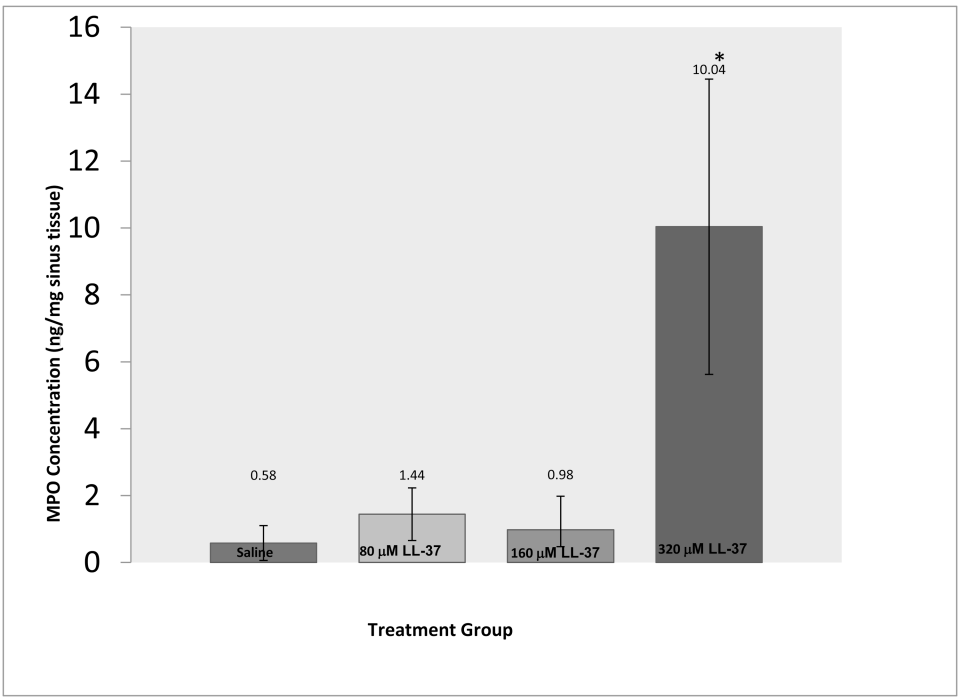


**Figure 4.**

A dramatic significant increase in MPO was observed with higher concentration of LL-37 in sinonasal challenged tissue ($p < 0.05$).

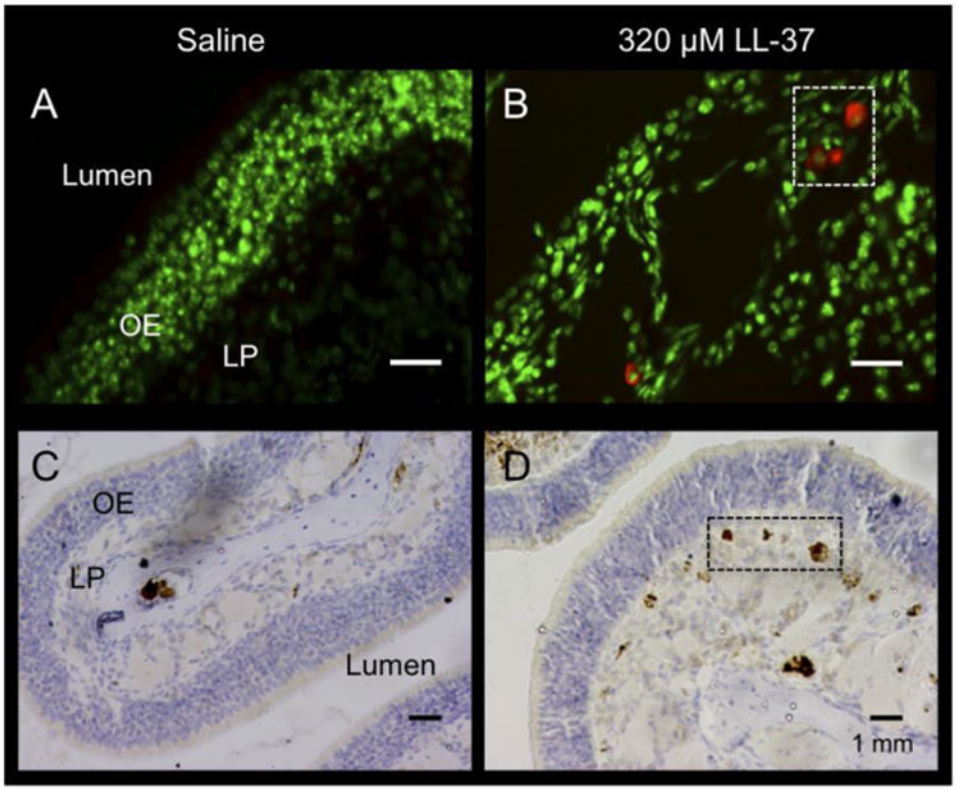


**Figure 5. Immunohistochemistry for mast cell tryptase**

Representative immunofluorescence (IF) (A & B) and immunohistochemistry (IHC) (C & D) for mast cell tryptase from saline (A & C) and 320 μM LL-37-treated (B & D) mice. Tryptase is represented by red staining, and nuclei are stained green (A & B). Boxes and dark brown areas indicate mast cells, as detected by tryptase-DAB stain (C & D). LP (lamina propria), OE (olfactory epithelium).

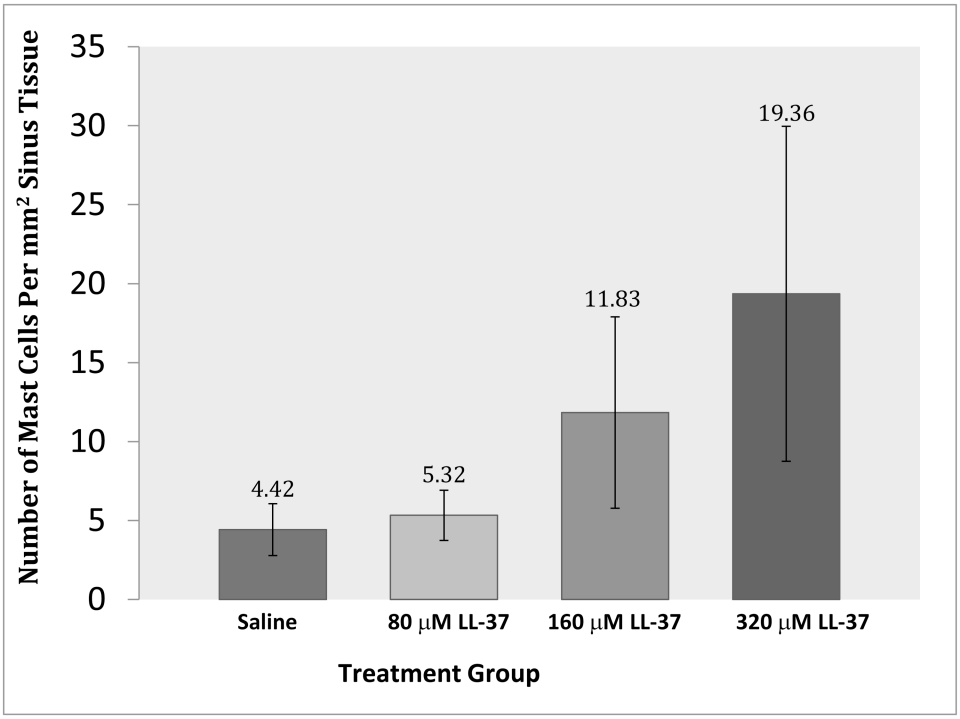


**Figure 6.**
Mast cells per $mm^2$ of tissue after LL-37 treatment.

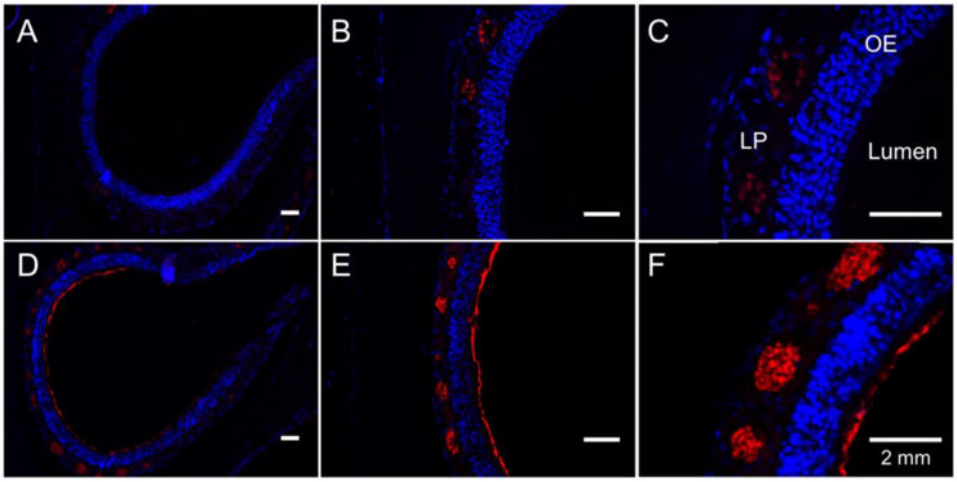


**Figure 7. Representative IF images following inoculation with fluorescently labeled LL-37**

(**A**), (**B**), and (**C**) represent tissues harvested 30 minutes after inoculation with LL-37 at 10×, 20×, and 40× magnification, respectively. (**D**), (**E**), and (**F**) represent tissues harvested 24 hours after inoculation at 10×, 20×, and 40×, respectively. Nuclei are counterstained with DAPI (blue). Red represents fluorescent LL-37. At 30 minutes, there is coating of the epithelial layer, as well as bright staining within the lamina propria. At 24 hours, there is absence of fluorescent LL-37 coating the epithelium with minimal evidence of fluorescent LL-37 present in the lamina propria. OE (olfactory epithelium); LP (lamina propria).

Author Manuscript

Author Manuscript

Author Manuscript

**Table 1**

**Severity of Inflammation**

| | Difference | P-value * |
|---|---|---|
| 80 μM LL-37 vs. Saline | 0.83(0.24~1.43) | 0.04 |
| 160 μM LL-37 vs. Saline | 1.53(0.94~2.13) | <0.001 |
| 320 μM LL-37 vs. Saline | 3.43(2.84~4.03) | <0.001 |
| 160 μM LL-37 vs. 80 μM LL-37 | 0.7(0.1~1.3) | 0.10 |
| 320 μM LL-37 vs. 80 μM LL-37 | 2.6(2~3.2) | <0.001 |
| 320 μM LL-37 vs. 160 μM LL-37 | 1.9(1.3~2.5) | <0.001 |

*Adjusted p-value using Tukey's method. All treatment pairs are significantly different from each other except for 160 μM LL-37 and 80 μM LL-37.

**Table 2**

**Lamina Propria Thickness**

| | Difference | P-value* |
|---|---|---|
| 80 μM LL-37 vs. Saline | 0.57(-0.11~1.24) | 0.32 |
| 160 μM LL-37 vs. Saline | 1.87(1.19~2.54) | <0.001 |
| 320 μM LL-37 vs. Saline | 3.27(2.59~3.94) | <0.001 |
| 160 μM LL-37 vs. 80 μM LL-37 | 1.3(0.63~1.97) | 0.003 |
| 320 μM LL-37 vs. 80 μM LL-37 | 2.7(2.03~3.37) | <0.001 |
| 320 μM LL-37 vs. 160 μM LL-37 | 1.4(0.73~2.07) | 0.002 |

*Adjusted p value using Tukey's method. All treatment pairs are significantly different from each other except for Saline and 80 μM LL-37.

**Table 3**

**Secretory Hyperplasia**

| | Difference | P value* |
|---|---|---|
| 80 μM LL-37 vs. Saline | 0.87(0.08~1.65) | 0.13 |
| 160 μM LL-37 vs. Saline | 1.93(1.15~2.72) | <0.001 |
| 320 μM LL-37 vs. Saline | 3.4(2.61~4.19) | <0.001 |
| 160 μM LL-37 vs. 80 μM LL-37 | 1.07(0.28~1.85) | 0.047 |
| 320 μM LL-37 vs. 80 μM LL-37 | 2.53(1.75~3.32) | <0.001 |
| 320 μM LL-37 vs. 160 μM LL-37 | 1.47(0.68~2.25) | 0.005 |

*Adjusted p value using Tukey's method. All treatment pairs are significantly different from each other except for Saline and 80 μM LL-37.

## Table 4

### Mast Cell counting

| | Saline | 80 μM LL-37 | 160 μM LL-37 | 320 μM LL-37 |
|---|---|---|---|---|
| Mean (SD) /mm$^2$ | 4.4 (1.6) | 5.3 (1.6) | 11.8 (6.1) | 19.3 (10.6) |
| Median (IQR) /mm$^2$ | 4.5 (0.8, 1.3) | 6.1 (5.2, 6.1) | 11.4 (7.0, 12.0) | 19.6 (10.5, 26.9) |
| Range /mm$^2$ | (2.6, 6.1) | (2.5, 6.6) | (7.0, 21.8) | (7.0, 33.2) |

Wilcoxon rank sum test p-value = 0.01, was used for LL-37 vs. Saline: the comparison LL-37 vs. Saline was significant in our test above.